

Characterization of a MEMS pressure sensor by a hybrid methodology

Ryszard J. (Rich) Pryputniewicz and Cosme Furlong
NEST – NanoEngineering, Science, and Technology
CHSLT – Center for Holographic Studies and Laser micro-mechaTronics
Mechanical Engineering Department
Worcester Polytechnic Institute
Worcester, MA 01609-2280 USA
E-mail: rjp@wpi.edu

ABSTRACT

Recent advances in surface micromachining and microelectromechanical systems (MEMS) technology have led to development of a new MEMS pressure sensor. In this sensor, pressure changes are detected by deformations of a diaphragm. This diaphragm is about 650 μm long, 160 μm wide, and about 2 μm thick, made of several different materials, each having different properties, especially different coefficients of thermal expansion (CTE). As a result, when the sensor is exposed to an environment, where in addition to pressure changes temperature changes also, measurements are adversely affected by its thermomechanical response. In addition, shape of diaphragms is also affected during fabrication. Objective of this study was to develop a hybrid, computational and experimental, methodology for characterization of behavior of MEMS pressure sensors (the methodology is also applicable to other sensors/structures as well). In our methodology, computational developments are based on a finite element method (FEM) and the experimental development is based on the state-of-the-art (SOTA) optoelectronic laser interferometric microscope (OELIM) method. Accurate and precise pressure measurements using MEMS sensors are limited not only by the effects that environmental temperature variation has on their performance, but also by the effects due to fabrication. As the sensor is exposed to changing pressures, the diaphragm deforms. Deformations of the diaphragm cause changes in resistance of the bridge circuit, which is an integral and critical part of the MEMS sensor. In this study the sensors were subjected to a differential pressure of ± 670 Pa (± 10 psig) at room temperature. Analyses were performed for the combined pressure and thermal loads. Ideally, the diaphragm should be absolutely flat when the sensor is at rest, i.e., at the atmospheric pressure. However, because of residual stresses due to fabrication, the diaphragms were irregularly deformed by up to 90 nm. Also, deformation nonlinearity, due to loadings by positive or negative pressure differences of the same magnitude, is vividly displayed by the OELIM measurements: the negative pressure difference yields the maximum deformation of 792 nm, while the positive one yields the magnitude of 813 nm, resulting in a difference of 21 nm, which is significant while interpreting the results. Comparison of computational and experimental results indicates good correlation and shows that the hybrid methodology is very effective for characterization of MEMS pressure sensors.

Keywords: MEMS, pressure sensors, differential pressure, hybrid methodology, uncertainty analysis, nanometer measurement accuracy, design by analysis.

1. INTRODUCTION

Demands for high performance, stable, and affordable sensors for applications in process control industry have led to development of a new miniature pressure sensor. This development, made possible by recent advances in MEMS, utilizes polysilicon-sensing technology. The unique *polysilicon piezoresistive sensor (PPS)* measures *differential pressure (DP)* based on deformations of a *multilayer/multimaterial diaphragm*, which is about 2 μm thick. Deformations of the diaphragm, subjected to changes in pressure, are sensed by the *piezoresistive bridge elements*, which are about 0.4 μm thick. Determination of the loading pressures from strains of the piezoresistors is based on computations relying on a number of material specific and process dependent coefficients that, because of their nature, can vary, which may lead to uncertainties in displayed results. To establish an independent means for measurements of deformations of the PPS diaphragms and to validate the coefficients used, we have developed a *hybrid methodology*, based on *optoelectronic laser interferometric microscopy (OELIM)* and *finite element method (FEM)* coupled with *uncertainty analysis (UA)* provided by unique closed form formulations. This methodology allows highly accurate and precise *nano-scale measurements* of displacements/deformations of diaphragms, as well as their *computational modeling/simulations*, and is the basis for “*design by analysis*” approach leading to efficient and effective developments of new MEMS sensors. In this paper we present this approach and illustrate its use by representative examples.

Advances in *single crystal sensor technology* made it become widely and successfully used in standard piezoresistive pressure sensors, in spite of the fact that it has a number of characteristics that limit its potential for future technological advancement [1]. The conventional single crystal sensors employ p-n junction isolation and etched silicon diaphragm formation. Junction and surface leakage plus parasitic components, such as unwanted capacitance, place limits on how much their long-term stability can be improved. Also, the etched diaphragm formation effectively limits the number of diaphragms (that can be fabricated on a single chip) to just one. The need for both cost reductions and sensor performance improvements has led to the development of polysilicon piezoresistive sensors.

2. POLYSILICON PIEZOREZISTIVE SENSORS

Polysilicon piezoresistive sensor (PPS) technology differs significantly from the single crystal technology and has a number of advantages. The polysilicon technology employs dielectric isolation as a result of a *silicon-on-insulator (SOI)* structure and, therefore, is not subject to junction leakage instability. In addition, polysilicon sensing diaphragms are deposited to a specific, controllable thickness with consistency that facilitates fabrication and enhances performance.

Because the polysilicon sensors use deposited diaphragms, the amount of etching is reduced in their fabrication. One key advantage of the reduced etch volume is the ability to place multiple sensing diaphragms on a single sensing chip. Therefore, the technology is versatile because it can provide *absolute pressure (AP)*, *differential pressure (DP)*, as well as *temperature (T)* sensing elements on a *single chip* [2], resulting in a *multivariable (MV) sensor*, Fig. 1. In this paper, we concentrate only on the design and analysis of the *DP sensor*, Fig. 2.

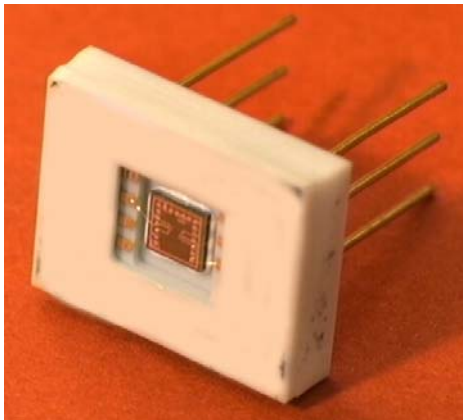


Fig. 1. MEMS polysilicon piezoresistive sensor package.

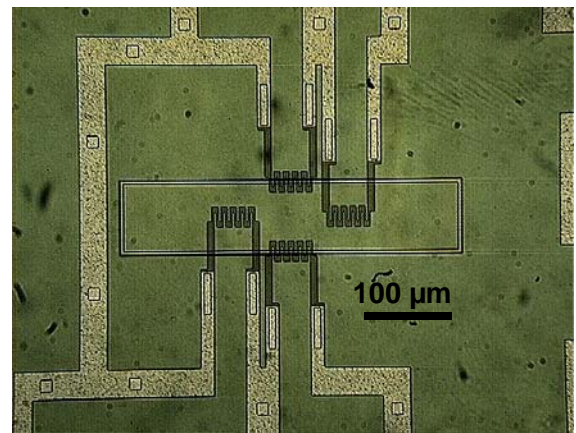


Fig. 2. Diaphragm of the DP sensor.

The diaphragm, Fig. 2, which senses the applied DP, is $160\ \mu\text{m}$ wide, $650\ \mu\text{m}$ long, and its *multilayer/multimaterial thickness* is about $2\ \mu\text{m}$. In this configuration, a backside pressure port is etched to $0.9\ \mu\text{m}$ deep cavity below the diaphragm. During functional operation of the sensor, deformations of the diaphragm are mechanically stopped by the bottom of the cavity giving the DP sensor a very large overage capability for the loads on high-pressure-side [3].

Deformations of the diaphragm are sensed by the piezoresistive bridge elements that are about $0.4\ \mu\text{m}$ thick. Determination of pressure from strains of the resistors is based on computations relying on a number of material-specific and process dependent coefficients that can vary because of variations in material and fabrication process control parameters, which may lead to uncertainties in displayed results. To establish an independent means for measurements of the PPS diaphragms and to validate the coefficients used, we have developed a hybrid methodology [4-6] for measurements and characterization of MEMS.

3. HYBRID METHODOLOGY

The hybrid methodology that we have developed for *measurements and characterization of MEMS* is based on OELIM and FEM coupled with UA provided by unique closed form mathematical formulations [4-9].

This methodology allows highly accurate and precise measurements of absolute and differential deformations of diaphragms as well as their computational modeling and simulation [10,11].

Configuration of the OELIM used in this study is shown in Fig. 3. In this configuration, a beam of collimated coherent light is brought into the system and is directed into a spatial filter (SF) assembly consisting of a microscope objective and a pinhole filter. The resulting (expanded) light field is then collimated by lens L1, and redirected by the directional beam splitter (DBS) through the long working distance microscope objective (MO) to illuminate the object/MEMS; the long working distance is required in order to accommodate fixtures/chambers (if needed) to subject the MEMS – or other objects – to specific, well controlled, loads. The proximal beam splitter (PBS) is placed close to the MEMS.

In this study, the MEMS sensors were placed in a specially developed fixture/chamber, Fig. 4, which facilitated reliable application of controlled pressure loads. The pressure loads could be applied to deform diaphragms toward the bottom of the cavity, or in the opposite direction, and readily identify the *high-pressure side (HPS)* and the *low pressure side (LPS)* of sensors, respectively.

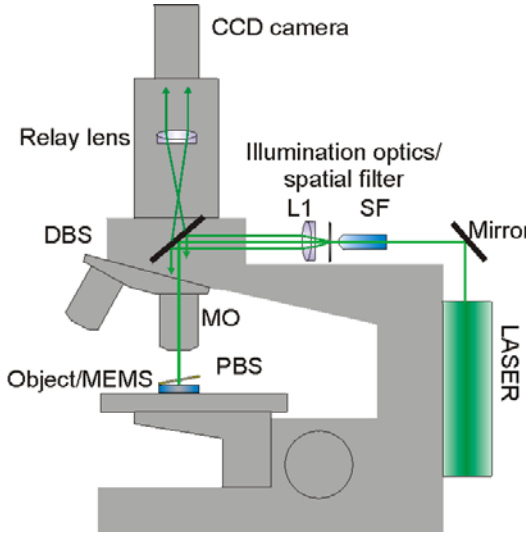


Fig. 3. OELIM system for studies of MEMS.



Fig. 4. Fixture/chamber for loading of the MEMS pressure sensors.

The proximal beam splitter (PBS) placed close to the pressure fixture/chamber provides, both, direct illumination of the MEMS PPS and a reference beam. The light reflected from the MEMS/object, together with the reference beam, are transmitted back through MO, DBS, and the relay lens to the CCD camera.

Images captured by the CCD camera are processed by a host computer to provide quantitative measurements of displacements/deformations of the diaphragms of the MEMS DP sensors. This processing is based on a relationship defining spatial distributions of intensity, $I_n(x, y)$, recorded by the CCD, i.e.,

$$I_n(x, y) = I_o(x, y) + I_r(x, y) + \sqrt{I_o(x, y)I_r(x, y)} \cos[\Delta\phi(x, y) + \theta_n + \Omega(x, y)] \quad , \quad (1)$$

where $I_o(x, y)$ and $I_r(x, y)$ represent intensities of the two interfering, i.e., object and reference, respectively, beams, $\Delta\phi(x, y)$ represents the optical phase difference between the two beams, and θ_n is the discrete phase step imposed during recording of the n -th image to facilitate determination of the fringe-locus function $\Omega(x, y)$, which relates to the displacements and the deformations. If $n = 5$, then from 5 relationships of the type of Eq. 1, we obtain [12]

$$\Omega(x, y) = \arctan \left\{ \frac{2[I_4(x, y) - I_2(x, y)]}{2I_3(x, y) - I_1(x, y) - I_5(x, y)} \right\} \quad . \quad (2)$$

The fringe-locus function determined from Eq. 2, in turn, relates to the unknown vectorial deformations $\mathbf{L}(x, y)$ via the equation [13]

$$\mathbf{K}(x, y) \bullet \mathbf{L}(x, y) = \Omega(x, y) \quad , \quad (3)$$

where $\mathbf{K}(x, y)$ is the sensitivity vector representing the OELIM geometry. Therefore, $\mathbf{L}(x, y)$ computed from Eq. 3 provides quantitative measurements of deformations of diaphragms of the DP sensors. Uncertainty, $\delta\mathbf{L}$, in this deformation can be determined using the following partial differential formulation [9]:

$$\delta\mathbf{L} = \left[\left(\frac{\partial\mathbf{L}}{\partial\mathbf{K}} \delta\mathbf{K} \right)^2 + \left(\frac{\partial\mathbf{L}}{\partial\mathbf{K}} \delta\mathbf{K} \right)^2 \right]^{\frac{1}{2}} \quad , \quad (4)$$

where δ indicates uncertainties, ∂ indicates partial derivatives, and the arguments (x, y) were omitted for simplification.

Maximum deformations of the diaphragm, L_{\max} , can be represented analytically as [14]

$$L_{\max} = \alpha \frac{pb^4}{Eh^3}, \quad (5)$$

uncertainty in which can be shown to be

$$\delta L_{\max} = \left[\left(\frac{\partial L_{\max}}{\partial \alpha} \delta \alpha \right)^2 + \left(\frac{\partial L_{\max}}{\partial p} \delta p \right)^2 + \left(\frac{\partial L_{\max}}{\partial b} \delta b \right)^2 + \left(\frac{\partial L_{\max}}{\partial E} \delta E \right)^2 + \left(\frac{\partial L_{\max}}{\partial h} \delta h \right)^2 \right]^{\frac{1}{2}}, \quad (6)$$

where α is the design parameter defining ratio of the length to the width dimensions of the diaphragm, b is the width of the diaphragm, h is its thickness, E is the modulus of elasticity of the material of the diaphragm, p is the applied pressure, and other symbols are as previously defined.

Computational modeling and simulation of the diaphragm displacements/deformations was based on the FEM model developed in this study, Fig. 5, using solid elements. Because of symmetry of the sensing element, Fig. 2, only half of the diaphragm was modeled in order to reduce computational time and to speed up the analysis. This model incorporates the multilayer/multimaterial structure of the diaphragm and accounts for specific material properties of each layer. It also incorporates the piezoresistive gauges and their operational characteristics.

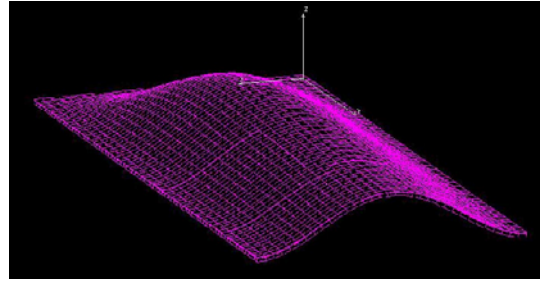


Fig. 5. FEM half-model of the MEMS DP sensor.

The deformations calculated using Eqs 3 and 5 were compared with the FEM results and their comparison with the corresponding uncertainties, based on Eqs 4 and 6, shows good correlation.

5. RESULTS AND DISCUSSION

Using the test fixture/chamber, the MEMS DP sensors were subjected to the HPS and the LPS loads. These loads ranged from the rest (i.e., reference) pressure, set as atmospheric, to ± 10 psig (± 670 Pa). Representative OELIM fringe patterns, corresponding to deformations of the diaphragms subjected to these loads, are shown in Figs 6 and 7.

It should be noted that the absolute shape (due to fabrication) of the diaphragms at rest, Fig 6a, influences its response to the applied pressures. That is, deformed shapes of the specific diaphragms were different under HPS and LPS loads of the same magnitude, as, e.g., can be seen in Fig. 7, which shows OELIM fringe patterns of a diaphragm subjected to the loads of zero psig, +10 psig, and -10 psig.

Based on prior studies [3] as well the intended design, deformations of the diaphragms due to HPS and LPS loads of the magnitudes shown in Fig. 7 are "unobstructed". Yet, the fringe patterns vividly indicate different deformation patterns. Clearly, changes in the OELIM fringe patterns display changes in the deformations of the diaphragms in response to the applied loads.

There are a number of ways to display quantitative results representing deformations of the diaphragms obtained from the OELIM fringe patterns. One way that facilitates comparison of deformations is to display them along, e.g., transverse lines similar to the line TT shown in Fig. 7a, which are summarized in Fig. 8 and indicate that deformation magnitudes increase with increasing loads. Also, deformation versus load as well as residual deformations of the diaphragms due to fabrication can readily be determined along longitudinal lines through centers of the diaphragms, such as the line LL in Fig. 7b. These

deformations (along the longitudinal lines) help to quantify nonlinear responses of the diaphragms to the loads of the same magnitude, but different directions of loading, which is indicated by the \pm signs in Fig. 9.

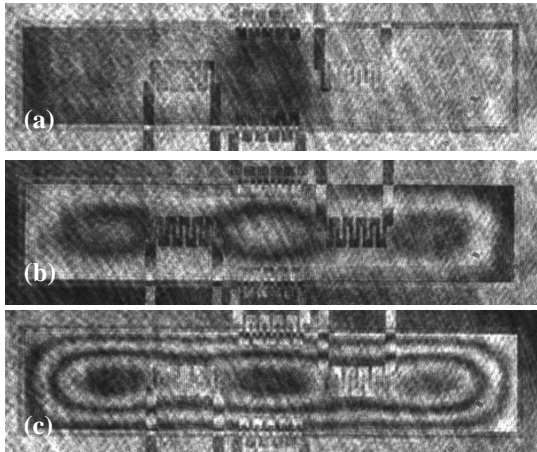


Fig. 6. OELIM fringe patterns of a DP diaphragm: (a) at rest, i.e., at zero psig, (b) diaphragm subjected to the differential pressure of +4 psig, and (c) the differential pressure of +10 psig.

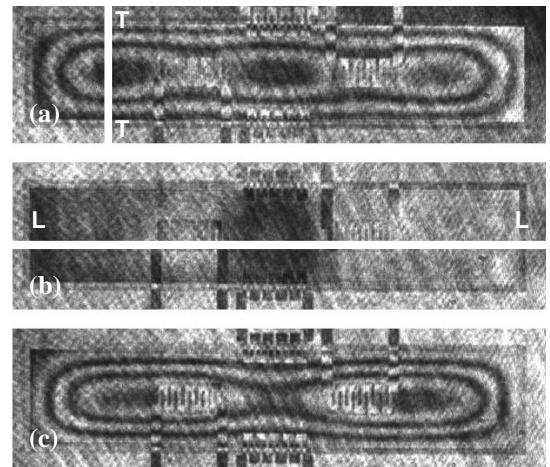


Fig. 7. OELIM fringe patterns corresponding to the absolute shapes of a DP diaphragm: (a) at +10 psig, (b) at rest, i.e., at zero psig, and (c) at -10 psig.

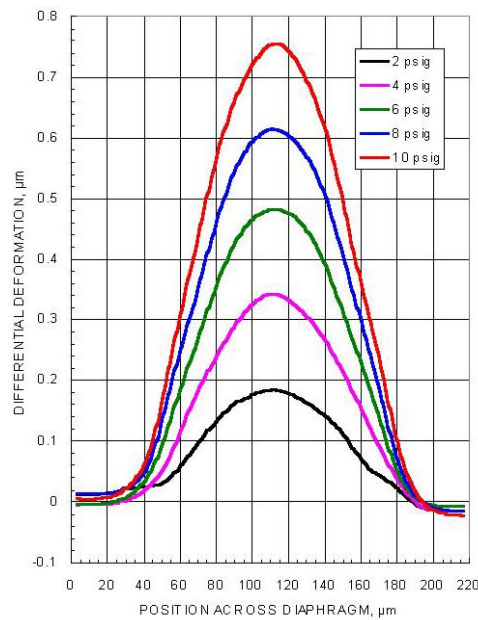


Fig. 8. Summary of differential deformations of a DP diaphragm along the line TT of Fig. 7a based on OELIM measurements, for several positive DP loads.

Figure 9 indicates that the deformations at rest range from -20 nm to +90 nm, for the DP diaphragms investigated herein; ideally, these deformations should be zero. Furthermore, at the differential pressures of +10 psig and -10 psig the deformations are +813 nm and -792 nm, respectively, showing a difference of 21 nm; ideally (i.e., based on the prevailing theories) there should be no difference – in the deformations due to positive and negative loads of the same magnitude – at all.

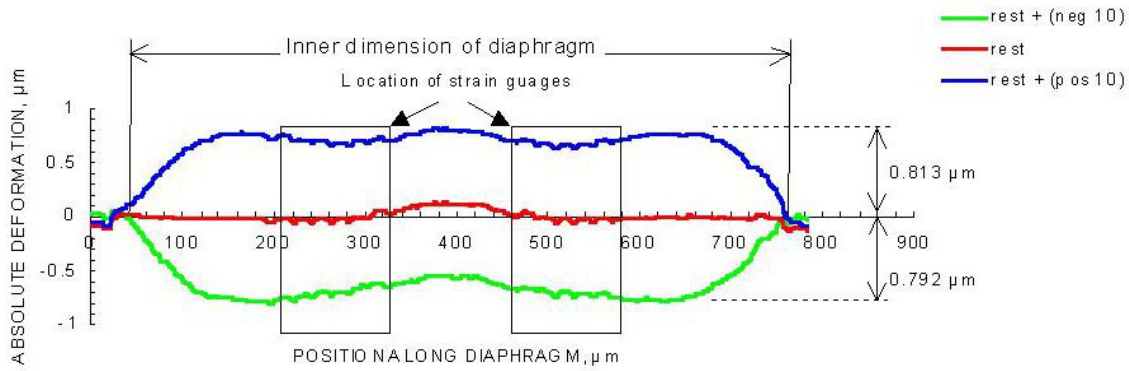


Fig. 9. Absolute shapes of a DP diaphragm along the line LL of Fig. 7b based on OELIM measurements at rest and at ± 10 psig loads, respectively.

Representative deformations and von Mises stresses based on FEM modeling are shown in Figs 10 and 11, respectively. Comparison of deformations measured by OELIM with those determined computationally using the FEM model shows good correlation, well within the uncertainties calculated using the analytical formulations of the hybrid methodology employed in this study. Continued development of correlations between the computational and the experimental results, coupled with analytically determined uncertainties, will be used to further validate procedures for accurate and precise determination of pressures based on deformations of the DP diaphragms. Furthermore, computational model of the DP diaphragms provides effective means for optimization of the design of the MEMS pressure sensors by parametric modeling, which allows efficient and effective considerations of geometry, dimensions, material properties, as well as *boundary, initial, and loading (BIL) conditions*.

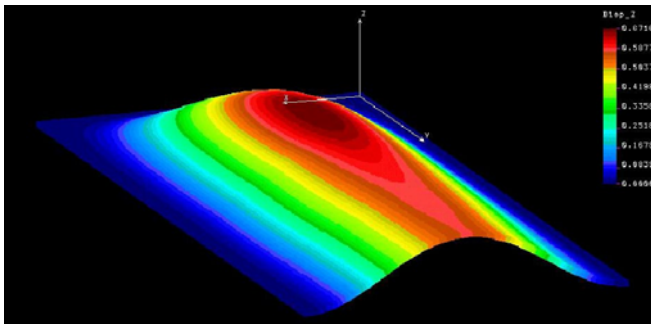


Fig. 10. Representative 3D deformations of a multilayer DP diaphragm subjected to the load of +10 psig, based on the FEM model shown in Fig. 5.

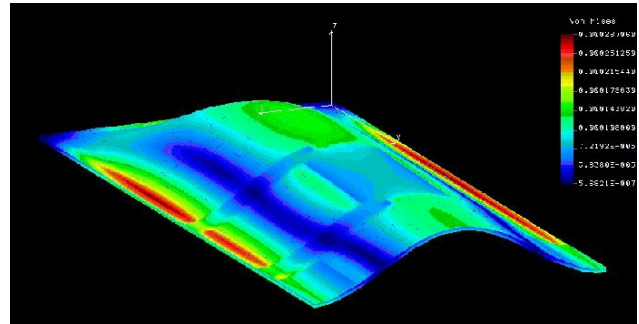


Fig. 11. Representative von Mises stresses of a multilayer DP diaphragm subjected to the load of +10 psig, based on the FEM model shown in Fig. 5.

6. CONCLUSIONS

MEMS PPS for measurements of DPs was described. Hybrid methodology for measurements and characterization of the pressure sensors was outlined. Preliminary results of the design by analysis of the sensor were presented.

Advances in the PPS technology permit fabrication of multiple cavities on a single chip allowing development of MV sensors. One of these sensors, considered herein, measures differential pressures based on deformations of a 2 μm thick diaphragm. In this paper, deformations of the diaphragms were studied using recently developed hybrid methodology, which is based on the SOTA optoelectronic laser interferometric microscopy (OELIM) and the finite element method (FEM) modeling coupled with the uncertainty analysis (UA).

The OELIM methodology provides measurements of displacements/deformations of diaphragms with submicron spatial resolution and nanometer measurement accuracy. The results of measurements indicate that due to fabrication processes the diaphragms are not flat, as it is ideally expected, but have residual deformations ranging from -20 nm to $+90$ nm. The results also indicate that operational deformations of the diaphragms are not symmetric with respect to their shape at rest, but are nonlinear. That is, these deformations are $+813$ nm and -792 nm when a diaphragm is subjected to the differential pressures of $+10$ psig and -10 psig, respectively, producing a difference of 21 nm; ideally there should be no difference in these measurements at all.

To develop an understanding of deformations of diaphragms subjected to specific BIL conditions, a FEM model was developed. Comparison of the OELIM and the FEM results shows good correlation, well within the analytically calculated uncertainties.

Development of the *hybrid methodology for design by analysis* of the MEMS sensors will continue and will be used to analyze and optimize, in an efficient and effective manner, new sensor designs for specific applications.

7. REFERENCES

1. Rowe, J. R., "Advanced sensor technology key to new multivariable transmitter," *Proc. Instr. Soc. Am.*, 1999.
 2. Pryputniewicz, R. J., Champagene, R. P., Angelosanto, J. P., Brown, G. C., Furlong, C., and Pryputniewicz, E. J., "Multivariable MEMS polysilicon piezoresistive sensor: analysis and measurements," *Proc. Internat. Symp. on Microscale Systems*, Orlando, FL, pp. 72-75, 2000.
 3. Pryputniewicz, R. J., Angelosanto, J. P., Furlong, C., Brown, G. C., and Pryputniewicz, E. J., "Analysis and measurements of high pressure response of MEMS sensors," *Proc. Internat. Symp. on MEMS: Mechanics and Measurements*, Portland, OR, pp. 76-79, 2001.
 4. Pryputniewicz, R. J., "A hybrid approach to deformation analysis," *Proc. SPIE*, 2342:282-296, 1994.
 5. Pryputniewicz, E. J., Angelosanto, J. P., Brown, G. C., Furlong, C., and Pryputniewicz, R. J., "New hybrid methodology for the development of MEMS multivariable sensors," *Paper No. IMECE2001/EPP-24722*, ASME – Am. Soc. Mech. Eng., New York, NY, 2001.
 6. Pryputniewicz, R. J., Hefti, P., Klemptner, A. R., Marinis, R. T., and Furlong, C., "Hybrid methodology for the development of MEMS," in press: *J. Strain Analysis for Engineering Design*, 2006.
 7. Furlong, C., *Hybrid, experimental and computational, approach for the efficient study and optimization of mechanical and electro-mechanical components*, Ph.D. Dissertation, Worcester Polytechnic Institute, Worcester, MA, 1999.
 8. Brown, G. C., *Laser interferometric methodologies for characterizing static and dynamic behavior of MEMS*, Ph.D. Dissertation, Worcester Polytechnic Institute, Worcester, MA, 1999.
 9. Pryputniewicz, R. J., *Engineering experimentation*, Worcester Polytechnic Institute, Worcester, MA, 1993.
 10. Brown, G. C., and Pryputniewicz, R. J., "New test methodology for static and dynamic shape measurements of microelectromechanical systems," *Opt. Eng.*, 39:127-136, 2000.
 11. Furlong, C., and Pryputniewicz, R. J., "Absolute shape measurements using high-resolution optoelectronic holography methods," *Opt. Eng.*, 39:216-223, 2000.
 12. Pryputniewicz, R. J., and Furlong, C., "Novel optoelectronic methodology for testing of MOEMS," *Proc. Internat. Symp. on MOEMS and Miniaturized Systems III*, SPIE-4983:11-25, 2003.
 13. Pryputniewicz, R. J., "Quantitative determination of displacements and strains from holograms," Ch. 3 in Vol. 68 of the Springer Series on Optical Sciences, *Holographic interferometry*, Rastogi, P. K., ed., Springer-Verlag, Berlin, pp. 33-72, 1994.
 14. Johari, H., *Development of a single package MEMS sensor for measurements of temperature, pressure, and relative humidity*, MS Thesis, Worcester Polytechnic Institute, Worcester, MA, 2003.
-